Program Digest, 2019 IEEE International Ultrasonics Symposium (IUS)
Glasgow, Scotland, October 6-9, 2019

Effects of Culture Conditions on Sonoporation of Dendritic Cells

Ryunosuke Matsumoto[1], Nobuki Kudo[2]
[1]*Graduate School and* [2]*Faculty of Infomation Science and Technology,*
Hokkaido University
Sapporo, Japan
kudo@ist.hokudai.ac.jp

***Abstract*—The presentation of an antigen for dendritic cells (DCs) is an important application of sonoporation to immunotherapy. To achieve efficient sonoporation of DCs, it is important to determine suitable conditions of cells (floating or adherent cells) and bubbles (phagocytosed or attached bubbles). In this study, the effects of the cell and bubble conditions on sonoporation were investigated using a high-speed camera and a confocal microscope. Two types of samples, DCs incubated on a coverslip for 0.5 h (quasi-floating cell sample) and DCs incubated for 48 h (adherent cell sample), were used to study the effects of cell conditions. Another two types of samples with different bubble conditions, phagocytosed and attached bubbles, were used to study the effects of bubble conditions. Areas of cell membrane adhesion on a coverslip scaffold, maximum expansion ratios and disappearance rates of bubbles, and membrane damage rates of cells were evaluated. The results indicated that the bubble expansion ratios and bubble disappearance rates were decreased in the condition of cells adhering to the scaffold and in the condition of bubbles being phagocytosed by DCs, resulting in decrease in a cell membrane damage rate.**

Keywords—Sonoporation, dendritic cell, immunotherapy, high-speed observation, confocal microscopy

I. Introduction

We have been studying sonoporation using pulsed ultrasound and microbubbles. Ultrasound exposure causes cell membrane perforation only at the locations of bubble adhesion, enabling transduction of drugs or genes that normally have no cell membrane permeability [1]. In recent years, much interest has been shown in immunotherapy in the field of cancer therapy, and electroporation has been clinically used as an technique for antigen presentation to dendritic cells (DCs) separated from a patient's blood [2]. Sonoporation has also been studied as an alternative technique that has higher levels of safety and efficiency in transduction [3]. DCs separated from a patient's blood are floating in a medium, whereas cells used in our previous studies [4] were adherent cells cultured on a scaffold. Since the morphologies of floating and adherent cells are different, ultrasound exposure conditions that are suitable for sonoporation might be different. Furthermore, DCs are known to have the ability to phagocytose microbubbles [5], suggesting that oscillation of phagocytosed bubbles might be different from that of bubbles adhering to the surface of DCs.

The purpose of this study was to investigate the effects of cell conditions (quasi-floating and adhering cells) and bubble condition (phagocytosed and attached bubbles) on sonoporation efficiency. Bubble dynamics under ultrasound exposure was observed using a high-speed camera, and resulting cell membrane damage was evaluated using a confocal microscope.

II. Materials and Methods

A. Dendritic cell samples

The murine DC line DC2.4 was used for experiments. In microscopic observation of cells irradiated by ultrasound, cells floating in a medium can easily move outside of a microscopic view field due to the radiation force of ultrasound, and it is difficult to identify the cells again to evaluate their damage. Therefore, DCs incubated on a coverslip for 0.5 h were used as quasi-floating DCs, and DCs incubated for 48 h were used as adherent DCs.

Microbubbles encapsulating C_3F_8 gas by a lipid shell labeled with nitrobenzoxadiazole (NBD) were used. Two-8 μL of a bubble suspension was added to 200 μL of Hanks balanced salt solution (HBSS) and the solution was dropped

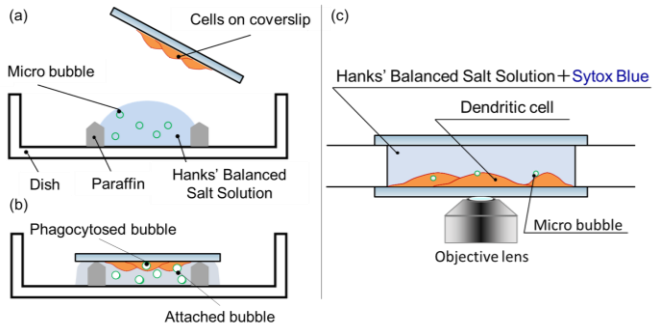

Fig. 1. Preparation of dendritic cell samples. (a) DCs were incubated on a coverslip. Hanks balanced salt solution (200 μL) supplemented with microbubbles was dropped into a 60-mm petri dish with paraffin spacers. (b) The coverslip was placed on the tops of the spacers to make bubbles attach to the cells. (c) The coverslip was attached to an observation chamber.

into a 60-mm petri dish with paraffin spacers (Fig. 1(a)). A coverslip seeded with DCs was placed on the tops of the spacers (Fig. 1(b)) with the cells facing down and incubated for DC sample was then attached to an observation chamber created on the bottom of a water bath (Fig. 1 (c)). The chamber was filled with 200 µL HBSS supplemented with 2 µL SYTOX Blue solution (5 mM). Before ultrasound exposure, both DCs with attached bubbles and DCs with phagocytosed bubbles were identified in the same microscopic view field. Ultrasound exposure was carried out after confocal observation to determine the bubble conditions

B. *Microscopic observation system*

An inverted-type microscope (Eclipse Ti, Nikon, Japan) with a water immersion lens (LWD Lambda S 40XC WI, Nikon, Japan) of N.A. = 1.15 and W.D. = 0.59-0.61 was used for observation of sonoporation phenomena. A high-speed camera (HPV-X2, Shimadzu, Japan) was connected to the right port of the microscope, and the bubble-cell interaction during sonoporation was visualized as a 256-frame video clip of bright field images captured at 5 or 10 Mfps.

A confocal microscope unit (C2si, Nikon, Japan) was connected to the left port, and the effect of ultrasound irradiation on DCs was investigated by confocal fluorescence microscopy before and after ultrasound irradiation. The fluorescence dye NBD (green) was used to visualize a bubble shell, Cellmask Orange (red) was used to visualize a plasma membrane, and SYTOX Blue (blue) was used to determine generation of cell membrane damage.

C. *Ultrasound exposure device*

The water bath was placed on the table of the microscope. A focused transducer with a diameter of 50 mm, focal length of 70 mm, and center frequency of 1.0 MHz was placed inside the bath. A sinusoidal burst pulse was generated by a function generator (AFG320, Sony Tektronix, Japan) and amplified by a wide band amplifier (UOD-WB-1000, Tokin, Japan) to drive the transducer. One shot exposure of a 3- or 100-cycle burst pulse of 1.0 MHz in center frequency and 0.2 or 0.6 MPa in peak negative pressure was used in the observations.

III. Results and Discussion

A. *Effects of cell conditions (quasi-floating and adherent cells)*

The first series of experiments was carried out to determine the effects of cell conditions using quasi-floating and adherent cell samples. Figures 2(a) and (d) show typical fluorescence images of a single cell visualizing adhesion of a plasma membrane to the coverslip. The adhesion areas of the membrane were 424 ± 219 µm^2 (n = 18) in adherent cells and 130 ± 79 µm^2 (n = 14) in quasi-floating cells, indicating that the cell conditions can be controlled by the incubation time after seeding ($p < 0.05$, Fig. 3(a)). The cells were then irradiated by a single shot of 3-cycle ultrasound pulse of 0.6 MPa in peak negative pressure, and the bubble oscillation was visualized as a 256-frame video clip (data not shown) captured at 10 Mfps to calculate the expansion ratio (maximum expansion diameter/initial diameter). The ratios were 5.0 ± 2.3

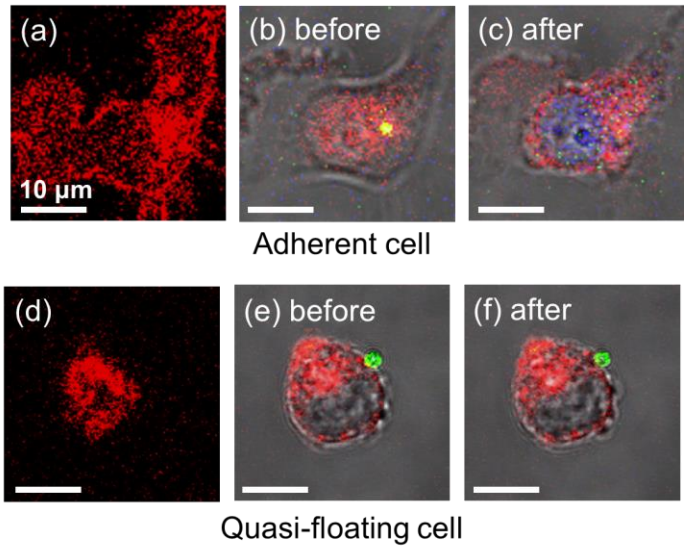

Fig. 2. Confocal images of dendritic cells: plasma membrane (Cellmask, red), bubble shell (NBD, green) and occurrence of membrane damage (Sytoxblue, blue). (a) An adherent cell before ultrasound exposure observed at a level just above the coverslip. The cell is firmly adhered to the scaffold. (b) The cell before ultrasound exposure. (c) The cell after ultrasound exposure. (d) A quasi-floating cell before ultrasound exposure observed at a level just above the coverslip. The cell is weakly adhered to the scaffold. (e) The cell before ultrasound exposure. (f) The cell after ultrasound exposure.

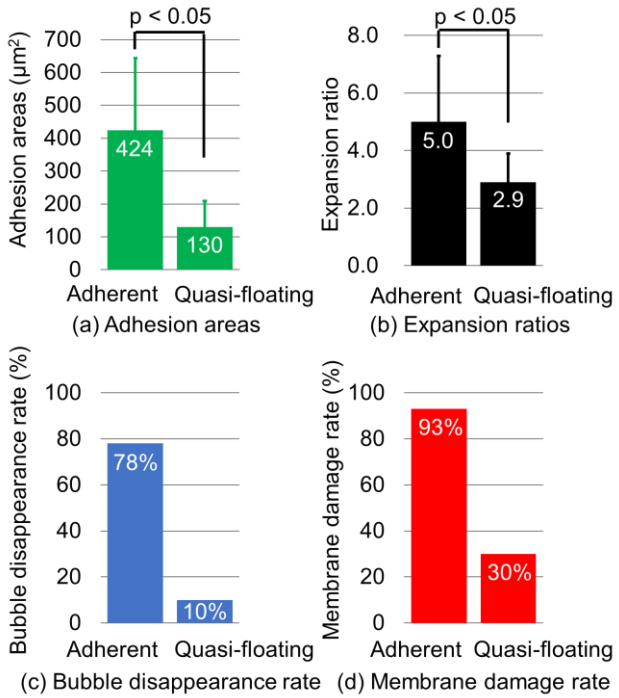

Fig. 3. Comparison of adherent and quasi-floating cell samples. (a) Areas of plasma membrane adhering to a coverslip scaffold. (b) Expansion ratios (maximum expansion diameter in the entire duration of the pulse/initial diameter). (c) Bubble disappearance rates, and (d) membrane damage rates.

in adherent cell samples and 2.9 ± 1.0 in quasi-floating cell samples, indicating that the cell condition can cause a significant difference in the amplitude of bubble oscillation ($p < 0.05$, Fig. 3(b)).

Figures 2(b) and (c) and Figs. 2(e) and (f) show microscopic images of the same cells before and after ultrasound irradiation. Each image shows an overlay of fluorescence on bright-field image. Figures 2(b) and (e) show membrane damage before ultrasound irradiation. Figures 2(c) and (f) show images after ultrasound irradiation. In the adherent cell sample, disappearance of bubble caused the appearance of blue fluorescence (Fig. 2(c)); however, intact bubbles was remained in the quasi-floating cell sample, and blue fluorescence was not observed (Fig. 2(f)). Disappearance of a bubble was found in 78% (11/14) of the adherent cells and in 10% (1/10) of the quasi-floating cells (Fig. 3(c)), and membrane damage was found in 93% (13/14) of adherent cells and in 30% (3/10) of the quasi-floating cells (Fig. 3(d)). All of the parameters shown in Figs. 3(b) to 3(d) had the same tendency of being higher in adherent cells and lower in quasi-floating cells, indicating that sonoporation of floating cells requires higher energy of irradiated ultrasound because floating cells absorb larger kinetic energy of the oscillating bubble.

B. Effects of bubble conditions (phagocytosed and attached bubbles)

The second series of experiments was carried out to investigate the effect of bubble phagocytosis on bubble dynamics. DCs with phagocytosed bubbles and DCs with bubbles attached to their surface were prepared using DCs incubated for 48 h to make adherent cell samples. The dependence of bubble dynamics on irradiated ultrasound energy was investigated using two ultrasound pulses of 0.2 MPa in peak negative pressure with durations of 3 cycles and100 cycles.

Figure 4 shows typical sonoporation phenomena induced

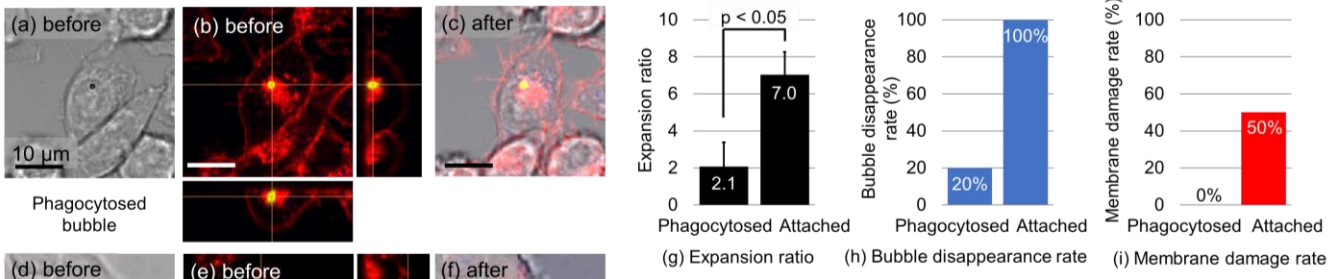

Fig. 4. Typical sonoporation phenomena induced by 3-cycle pulse exposure. (a) A bright-field image and (b) a confocal image before ultrasound exposure to a cell with a phagocytosed bubble. (c) A bright field image superimposed with a confocal image after ultrasound exposure. (d) A bright-field image and (e) a confocal image before ultrasound exposure to a cell with a bubble adhering to its surface. (f) A bright field image superimposed with a confocal image after ultrasound exposure. (g) Bubble expansion rates calculated using high-speed images of the entire duration of the 3-cycke pulse, (h) bubble disappearance rates, and (i) membrane damage rates.

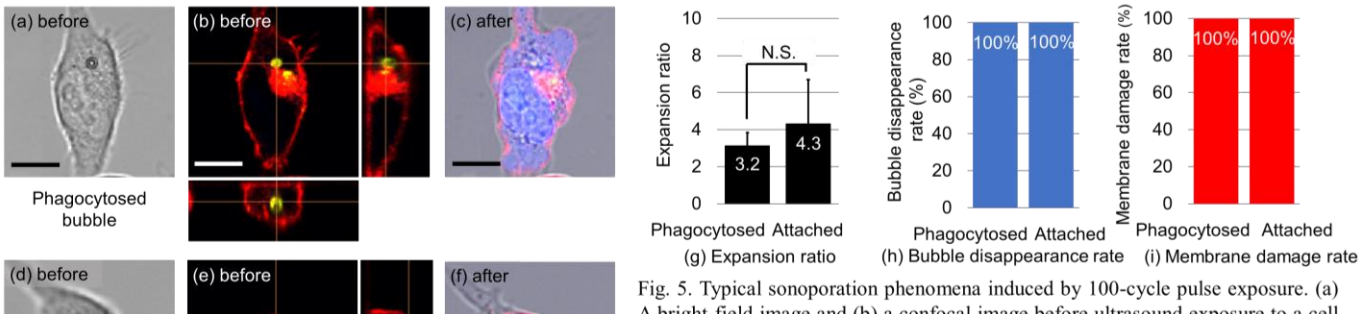

Fig. 5. Typical sonoporation phenomena induced by 100-cycle pulse exposure. (a) A bright-field image and (b) a confocal image before ultrasound exposure to a cell with a phagocytosed bubble. (c) A bright field image superimposed with a confocal image after ultrasound exposure. (d) A bright-field image and (e) a confocal image before ultrasound exposure to a cell with a bubble adhering to its surface. (f) A bright field image superimposed with a confocal image after ultrasound exposure. (g) Bubble expansion rates calculated using the high-speed images in the first 10 cycle of the 100-cycle pulse, (h) bubble disappearance rates, and (i) membrane damage rates.

by 3-cycle pulse exposure, and Fig. 5 shows those induced by 100-cycle pulse exposure. In each figure, the three images in the upper row show a DC with a phagocytosed bubble (a), (b) before and (c) after sonoporation, and the three images in the lower row show a DC with an attached bubble (d), (e) before and (f) after sonoporation. The graphs in (g) and (h) show the expansion ratios and disappearance rates of bubbles, and the graph in (i) shows the membrane damage rates of cells. The expansion ratio was derived from high-speed movie clips captured at 10 Mfps (3-cycle pulse) and 5 Mfps (100-cycle pulse), and the bubble disappearance and cell membrane damage rates were determined from the images in (c) and (f).

As shown in Fig. 4(g), the expansion ratios under the condition of exposure to a 3-cycle pulse were 2.1 ± 1.3 ($n = 5$) in the cell with a phagocytosed bubble and 7.0 ± 1.2 ($n = 4$) in the cell with an attached bubble, indicating significant suppression of bubble oscillation inside a cell ($p < 0.05$). Furthermore, the low bubble disappearance rates of 20% (1/5) for phagocytosed bubbles (Fig. 4 (h)) and the low membrane damage rate of 0% (0/6) for cells with a phagocytosed bubble (Fig. 4(i)) suggest that bubble phagocytosis increases absorption of kinetic energy during bubble oscillation that results in a decrease in membrane damage rate.

Condition to exposure to a 100-cycle pulse, the bubble expansion ratios of phagocytosed and adherent bubbles were 3.2 ± 0.7 ($n = 11$) and 4.3 ± 2.4 ($n = 10$), respectively, showing no significant difference (Fig. 5(g)). The bubble disappearance rates and membrane damage rates were 100% in all cell and bubble conditions (Figs. 5(h), (i)). The results indicate that large amplitude oscillation of a phagocytosed bubble causes transmembrane movement of the bubble that results in bubble disappearance and cell membrane damage.

IV. Conclusion

In order to investigate the effects of cell conditions (quasi-floating and adhering cells) and bubble conditions (phagocytosed and attached bubbles) on sonoporation efficiency, bubble dynamics and resulting cell membrane damage were visualized by high-speed and confocal microscopic observations. The results showed that a floating cell condition and a phagocytosed bubble condition decrease the bubble expansion ratio and the bubble disappearance rate, leading to a decrease in cell membrane damage rate.

Acknowledgment

This work was supported by JSPS KAKENHI Grant Number 17H00864.

References

[1] N. Kudo, K. Okada, K. Yamamoto, “Sonoporation by single-shot pulsed ultrasound with microbubbles adjacent to cells,” Biophysical Journal, vol. 96, pp. 4866−4876, June 2009.

[2] G. Schuler, B. Schuler-Thurner, R. M Steinman, “The use of dendritic cells in cancer immunotherapy,” Current opinion in immunology, vol. 15, 138-147, April 2003.

[3] Y.W. Han, A. Ikegami, P. Chung, L. Zhang, C.X. Deng, “Sonoporation is an efficient tool for intracellular fluorescent dextran delivery and one-step double-crossover mutant construction in Fusobacterium nucleatum,” Appl. Environ. Microbiol, vol. 73, pp. 3677-3683, April 2007.

[4] N. Kudo, Y. Kinoshita, “Effects of cell culture scaffold stiffness on cell membrane damage induced by sonoporation,” Journal of Medical Ultrasonics, vol. 41, pp. 411-420, March 2014

[5] G. Bioley, P. Bussat, A. Lassus, M. Schneider, J Terrettaz, B. Corthésy, “The phagocytosis of gas-filled microbubbles by human and murine antigen-presenting cells,” Biomaterials, vol. 33, pp. 333-342, January 2012.